PROGRESS IN COLOR, COLORANTS AND COATINGS

available online @ www.pccc.icrc.ac.ir

Prog. Color Colorants Coat. 13 (2020), 143-154

Ministry of Science, Research and Technology
Institute for Color Science and Technology

Energy Gap Demeanor for Carbon Doped with Chrome Nanoparticle to Increase Solar Energy Absorption

R. N. Abed*, N. K. Al-Sahib, A. J. N. Khalifa,
Mechanical Engineering, Engineering College, Al-Nahrain University, P.O. Box: 14022, Baghdad, Iraq.

ARTICLE INFO

Article history:
Received: 12 Jan 2019
Final Revised: 03 Aug 2019
Accepted: 21 Jun 2019
Available online:24 Nov 2019

Keywords:
Characterization of catalyst
Spray pyrolysis coating
Semiconductor synthesis
XRD measurements
FT-IR measurements.

ABSTRACT

Novel method doped carbon with nanoparticle Cr_2O_3 and thin film has been studied in much thought in wavelength range, the doping can help new excellent physical and chemical properties for carbon, this application has a semiconductor feature. Nanocomposite thin film deposited on copper and glass substrates have been created by utilizing Spray Pyrolysis method. The precursor solution for the nanocomposite (Cr_2O_3/C) was blended with the polyethylene glycol as a colloidal. The optical band gap is a crucial property for the nanocomposite, for instance, nanocomposite thin film of Cr_2O_3/C was kept by shower process on glass and copper substrates. The band gap for the nanocomposite photo-catalytic has been finished using X-ray diffraction, UV-Vis spectrometer. The assessed optical band gaps for direct and indirect transition values determined and were 3.5, 3.25 eV and photon energy 1.65 eV to carbon doped by nanoparticle Cr_2O_3. Thin film thickness ranging between 45-160 µm This paper achieved the doped carbon by nanoparticles of Cr_2O_3 for thin layer coating in flat plate collector. New coating activity may be given by novel nanocomposite Cr_2O_3/C structure as a semiconductor. Results showed a new nanocomposite to enhance the absorption of the solar energy light activity. Prog. Color Colorants Coat. 13 (2020), 143-154© Institute for Color Science and Technology.

1. Introduction

After Studies and applications in nanomaterial's are attracted in enormous consideration in both principal, because of their novel physical and chemical properties to dope the change metal particles to product, photo-catalytic forms can possibly yield real strides forward in most eminently in taking care of clean energy demand and handling the natural contamination [1-6]. The advancement of successful semiconductor photo-catalysts has in this manner rise into a standout amongst the most critical objectives in materials science [7].

For a long time, the most inquired about the nanoparticles material is Cr_2O_3; it has given the most proficient photo-catalytic action, highest stability, least cost and most minimal danger [8,9]. Study the characteristics of CNT synthesis throughout the thermal decomposition on a catalyst Ni/MgO by microwave radiation to increase the surface area for the catalyst from 5.2 to 9.1 m^2/g and study the microwave radiation effect on the catalyst to improve its efficiency for the nano product [10-14].

Progress metal oxide NPs has numerous applications as catalyst in solar energy conversion [15], superconductors [16] and absorbents. The Eg amounts specified and were from 2.34 to 2.40 eV for virgin and doped TiO_2 particles with copper. It was utilized for photo-degradation of amido black dye in water [17-21].

*Corresponding author: rasheednema@eng.nahrainuniv.edu.iq
rasheednema@yahoo.com

Metal-oxides constitute an essential class of materials that are associated with natural science, chromium oxides have pulled in much consideration as of late due to their significance both in science and innovation. Uncommon consideration has been concentrated around the arrangement and properties of chromium oxide (Cr_2O_3), which is essential in particular, connected applications, for example, it has resistance for high-temperature [22], it has corrosive resistance, green color [23], and catalysts [24]. It is significant that characteristic properties incredible activities have been committed to the examination of various Cr_2O_3 materials combination [25]. It gives high surface zone and particular partiality for absorption in composite.

Nanoparticles Cr_2O_3 gives promising developments to compound; energy growth as a result of its strong of photons that produced in holes, recently, a broad thought has been focused around assembling particular Cr_2O_3 nanoparticles [26, 27]. The Cr_2O_3 Nanoparticles have been made by various techniques including sol-gel, PVD, CVD, and co-precipitation [28].

It is remarkable that respectable metals have unique electronic and reactant properties, for example, examined its observable light activity for the photo-catalyst of regular blends [29]. The carbon doped by Cr_2O_3 nanoparticles organized to a raised temperature and unmistakably showed the capability of the Nanocomposite Cr_2O_3/C under evident light illumination. Further, to produce a good absorption for this coating under solar light [30].

The absorption inspected of materials inside carbon nanotubes can be invested in tube tips, sidewalls, and central zones of the empty spaces. Nanotubes can give a generous specific surface district and a strong van der waals restricting energy on all around showed retention goals [31]. Nanoparticle Cr_2O_3 doped TiO_2 and investigated by using no contact nuclear power microscopy (NC-AFM). This happens to constitute strong proof for improvement surface opportunity through chromium for doping of TiO_2 [32].

By using the oblique angle co-deposition to deposit particularly balanced assortments of Cr/TiO_2 composite nano rods of TiO_2 that show optical properties in the detectable district. The effect of the Cr particles to dope TiO_2 and exhibit the optical into the TiO_2 cross section [33, 34]. Thin films of Cr doped TiO_2 store on porous silicon from electrochemical anodization of multi-crystalline Si wafers. The effect of Cr doping on the properties of the TiO_2-Cr/PS/Si tests has been inspected by strategies for X-ray diffraction (XRD), atomic power microscopy (AFM), photoluminescence (PL) lifetime. Cr-doped TiO_2 films were prepared using the sputtering deposition technique. The point for this work involves redesigning the undeniable light ingestion of the TiO_2 films through Cr doping, while TiO_2 was ingesting obliged an energy radiation as high as 3.2 eV [35].

Photo-catalyst composite coatings of Cr-TiO_2 on alumina (Al_2O_3) balls had been set up with Ti powder including a particular substance of Cr powder about oxidation process. The effect of these conditions on the structure for photo-catalytic development under UV to redesign photo-catalytic activity by adding Cr to TiO_2 as a coating for the alumina balls [36].

The band gap arranged to deal with and find photo-catalytic semiconductor chooses to improve the photo-catalytic activity of it [37]. The adequacy of photo-catalytic activity depends upon high optical absorption. Most semiconductors have band gap regards more than 3.0 eV, at that point it band hole arranged at around 3.2 and 3.0 eV, exclusively. Along these lines, light is just consumed by the dye. The authorized electron is moved into the conduction band of the semiconductor forsaking a hole limited on the dye [38].

Essentially, there are two sorts of optical progress that can happen at the principal edge of crystalline semiconductors: direct or indirect advances. Hence, the types of the assimilation coefficient α as a component of photon energy (Eg= hν) rely upon the energy of bands. For basic allegorical groups for circuitous progress ($(E_g\alpha)^2$ and $(\alpha E_g)^{1/2}$) [39].

Numerous methods to make thin film, one of these methods was spray pyrolysis to prepare thin film coating on substrate, because of straightforward to dope film, at any stage don't need vacuum to deposit coating applications, eliminates the main drawbacks of chemical ways like sol-gel that produces films of restricted thickness, and it producing thickness of the films at different rate of deposition. The thickness of film depends on the distance between the substrate and spray orifice, temperature of substrate, the concentration of solution sprayed and droplet landing [40].

In this paper Cr_2O_3/C, nanocomposite photo-catalysts were first integrated to demonstrate obviously to light responding. These open entryways for the change photo-catalysis through carbon doped by nanomaterial, for instance, Cr_2O_3 that showing the applications to begin a mix technique to estimation of photo-catalytic activity. This has been viewed as a remarkable semiconductor photo-catalyst as a result of its execution. Undoubtedly, photo-catalysis utilizing by carbon doped by Cr_2O_3 to make another semiconductor for setting up another material that absorbed solar energy, when used as a coating on the flat plate collector and absorbed the solar energy. The novelty to manufacture cheap coating by utilizing carbon doped with Cr_2O_3 to producing a semiconductor and without made a coating from nanomaterial's only have high cost.

2. Experimental

2.1. Catalyst characterization

The specimens arranged by blended carbon and Cr_2O_3 nano powder to be as a colloidal used in spray coating. The XRD diffraction equipment was SHIMATZU (CU-Kα1), radiation source (λ= 1.5406 Å) at 30 Kv and 20 mA, used to decide the compositions and precious crystal structures. The surface morphologies and cross-sectional microstructures of the examples were measured. The optical absorption spectra of the composite were recorded utilizing SHIMATZU 1650 PC UV-VISIBLE spectrophotometer for the samples, with a wavelength range of 200–800 nm.

The FT-IR spectrophotometer is a SHIMADZU FTIR-8300 FOURIER TRANSFORM INFRARED SPECTROMETER, it's wavelength from (200-4000 cm^{-1}) for spectral band width (2 cm^{-1}).

2.2. Chromium Oxide Nanoparticle

The purity of Cr_2O_3 (99.9%, normal distance across of 18.51 nm) and nanoparticle size of Cr2O3 is (18.51 nm) when inspected by AFM device, Figure 1 clarified the diameter of the particles and AFM picture in 3D dimension

2.3. Carbon Particles

Carbon have been set up from the market and working some procedure on it from: granulating and sieving to accomplish small scale molecule at that point taking EDS for the carbon molecule we find that the measurement of the molecule between (20.51-140.0 μm) was clarified in Figure 2.

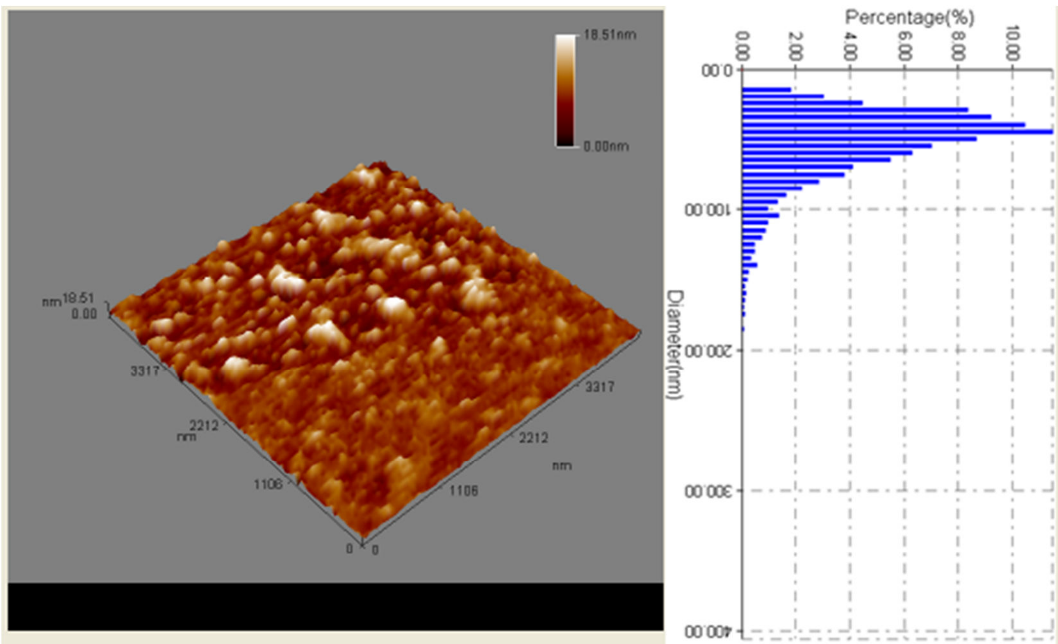

Figure 1: Size of Cr_2O_3 nanomaterial by AFM device.

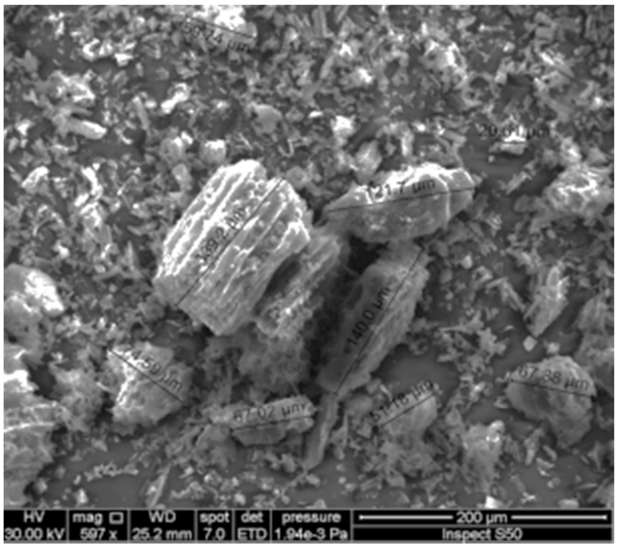

Figure 2: Carbon EDS by SEM equipment.

So, the carbon powder gotten by a process after isolating it in a sifter (550 µm), then grindery the carbon and isolating it in the sifter (125 µm) and by SEM surveying the particle of the carbon and it find around (20.51-140 µm) shown in Figure 2. The carbon was sieving by a strainer (75 µm) and the atoms were around (2.592-25.48 µm), clarified in Figure 3. The EDX for the carbon specified from the SEM equipment and determined the composition of the carbon.

2.4. Synthesis Colloidal sol utilized in spray coating

The Wt% of Cr_2O_3 with carbon was added to polyethylene glycol (PEG 400) to set up the colloidal before were the colloidal blended for (1 h) by a stirrer to ensure the creation of a Cr_2O_3/C composite. The composite scattered in PEG400 with add distilled water to PEG400 in the lab at room temperature, after that place it in the glass tube to start in coating the specimens by spray pyrolysis method. This equipment clarified in the Figure 4. The air blower was utilized in the spray coating to blow the air under the activity of spray process.

In the beginning of the spray procedure through the glass tube the colloidal pour from the hole in the top of the tube glass over, then will be showered on the samples through the glass tube.

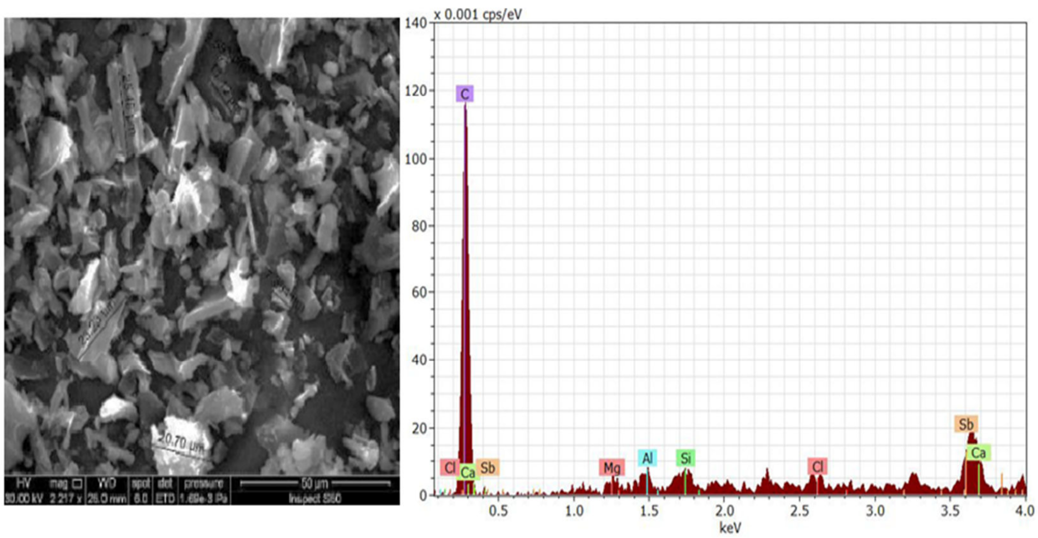

Figure 3: SEM-EDX for carbon in final stage.

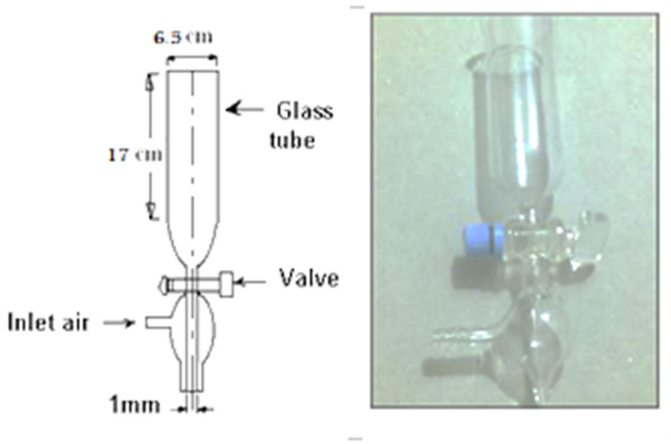

Figure 4: Spray pyrolysis equipment .

This glass chamber worked as a vacuum to show the effect inside the glass chamber to allow air to blend with colloidal beads in the end of a capillary tube to shower the colloidal on the samples. The air inters the side hole and meeting the beads of the colloidal toward the capillary tube to change the air pressure inside the glass cone. The spray cone shape implements on the samples that will be under the sprinkle space, the sample size was ($2.5\times 2.5 \times 0.2$ cm^3) was from the glass and copper as substrates. The sample puts under the atomizer, then putted underneath variation heater to enabling the sample to warming before begin in spray technique. The distilled water and PEG400 will vaporize under warming and samples will be dry. When completed the test; the dried samples puts in the furnace at temperature (250 ^oC) for (6 h) to guarantee the crystallization of the composite and leave them in the furnace to the next day when turning off the furnace.

2.5. Spectrally selective coatings for synthesis semiconductor (SSCs)

A novel design by utilizing Cr_2O_3/C nanocomposite as a semiconductor material that used as a coating for spectrally selective coatings (SSCs) on the surface of the flat plate collector. It is required to yield the light absorptivity in VIS–NIR extends because of the inherent band gap of nanocomposite Cr_2O_3/C (3.5 eV) for direct allowed transition and (3.25 eV) for indirect allowed transition. The carbon doped by using nanoparticle from Cr_2O_3 in the covering is exceptionally advantageous for spectrally selective coatings (SSCs) applications. Spray coating was utilized to deposit the Cr_2O_3/C onto a cleaned copper substrate (Cu) surface and glass. The nanocomposite (Cr_2O_3/C) particles were scattered in a natural dissolvable, for example, (PEG 400), and blending to make a uniform colloidal. The film thickness was controlled from (45 to 160 μm) by modifying the shower covering conditions; this was inspected by SEM device. The film thickness compared by a great company, for example the ALMICO Company that analyzed its film thickness for covering by TiO_2.

3. Results and Discussion

3.1. SEM measurements

The SEM picture shows nanocomposite Cr_2O_3/C as a semiconductor from tests, Figure 5 indicate nanocomposite layer after coating on the samples. The thickness of the produced films was (45-160 μm) measured using SEM (Scanning Electronic Microscope: Inspect S50), where the thickness was produced films of Cr_2O_3 doped Carbon when precipitated on glass films.

3.2. XRD measurements

The nanocomposite Cr_2O_3/C has been precipitated at room temperature on the samples and tested by utilizing X-ray diffraction equipment. The XRD demonstrates pinnacles of nanoparticles Cr_2O_3 and carbon before and after spray method for the samples are impressively expanded are appeared in Table 1. This expansion of XRD test does not make any change, this prove that the nanocomposite is a semiconductor because the position of the angles for the nano powder, carbon and the nanocomposite are the same before and after the coating (Figure 6).

The Table 1 displays the crystalline size (D) in Angstrom and the diagram represents polycrystalline of the Cr_2O_3/C that scored in the diagram, the crystalline size was calculated according to Debye-Scherrer formula and the diffraction heights consequently obtained from X-ray diffraction data that obtained from doping [42].

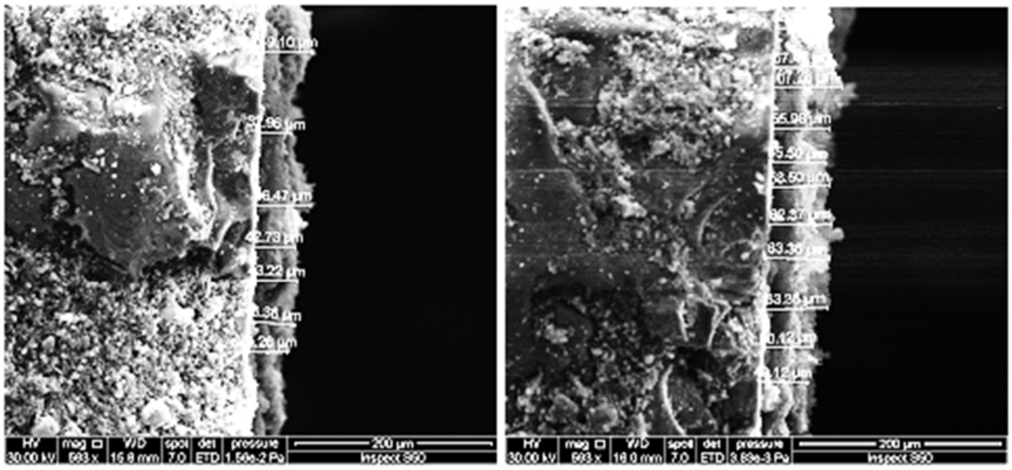

Figure 5: Nanocomposite film thickness .

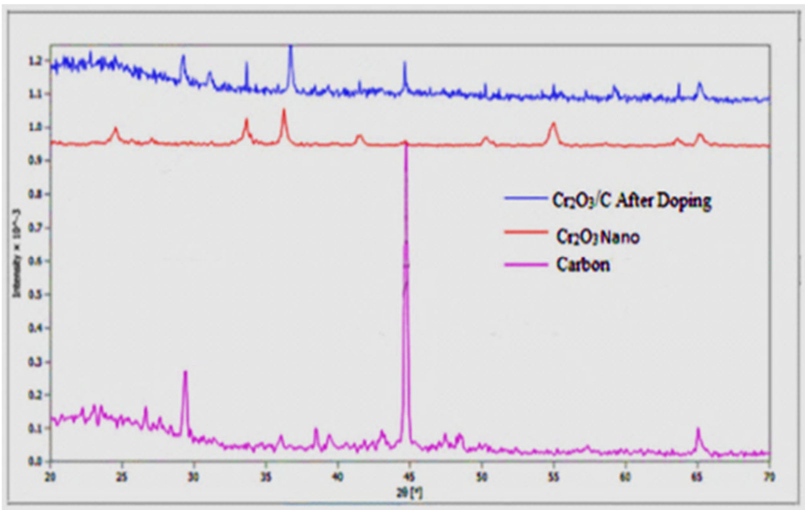

Figure 6: Nanocomposite (Cr_2O_3/C) before and after doping.

Table 1: Peaks of crystalline size for nanocomposite Cr_2O_3/C before and after doping.

NO.	2Theta (deg.)	D (A^o)	I/I_1	FWHM	Intensity (counts)
1	22.80	3.89	12	0.155	12
2	31.12	2.87	37	0.23	36
3	33.13	2.70	10	0.09	10
4	36.72	2.44	100	0.23	97
5	44.71	2.03	28	0.22	27
6	55.49	1.65	15	0.16	15
7	65.15	1.43	39	0.26	38

The particle size was calculated using the Scherrer's formula as [41] (Eq. 1):

$$D = 0.9\lambda / \beta \cos\theta \quad (1)$$

Where D is the normal molecule estimate opposite to the reflecting planes, (λ) is the X-ray wavelength, (β) is the full width at half maximum (FWHM), and (θ) is the diffraction point.

The Absorption coefficients (α), (Io) measured as the capacity of the energy of photon incident. Equation 2 depends on the Beer-Lambert law for optical absorption, (I) the transmitted light of the film with thickness (t), absorbance (A), and the absorption coefficient (α) which appeared in the accompanying condition [43]:

$$\alpha = \frac{1}{t} * ln(\frac{Io}{I}) = 2.303 \ \frac{A}{t} \ldots \quad (2)$$

3.3. Band gap energy analysis

The absorbance versus wavelength follows for the sum total of tests have been recorded in the range 300-800 nm as appeared in Figure 7. The absorption, which relates to electron excitation from the valence band to conduction band, can be utilized to decide the nature and estimation of the optical band gap. The connection between the absorption coefficients (α) and the incident photon energy (hν) can be composed as. The energy gap calculated from the optical band gap of the thin film for nanocomposite Cr_2O_3/C from the equation 3 [44, 45]:

$$h\nu \times \alpha = A \times [\ h\nu - Eg\ ]^n \quad (3)$$

Where (h) is the Planck constant (6.63 E-34), (ν) is the frequency (HZ (1/s)), Eg is the optical energy hole and A is exact consistent and exponent n relies upon the kind of progress. For direct allowed (n = 1/2), indirect allowed transition (n = 2).

To quantify the energy band hole from the absorption spectra a diagram $(\alpha h\nu)^2$ versus (hν) is plotted. The extrapolation of the straight line gives the estimation of the energy band hole. At that point from the resultant of the Cr_2O_3/C, found that the direct allowed band gap estimations of Cr_2O_3/C have been observed to be (3.5 eV) for direct transition, (3.25 eV) for indirect transition and the photon energy is (1.65 eV). At that point the outcome from the information of the results was shown in Table 2.

Table 2: Nanocomposite transition (direct and indirect) .

Direct	Indirect	Photon Energy
3.5 eV	3.25 eV	1.65 eV

Then the Figures 8 and 9 show the result of the data for the direct, indirect transition and photon energy for a band gap to the nanocomposite Cr_2O_3/C. The optical properties of the thin film for the nanocomposite are measured in the wavelength from (300-800 nm). The band hole is dictated by the reflection UV-Vis spectra of Cr_2O_3 doped carbon appeared in Figures 8 and 9 [46, 47].

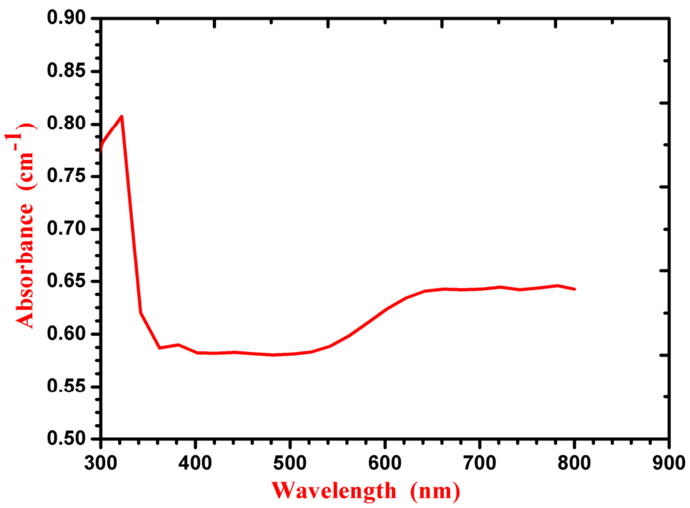

Figure 7: Absorbance of nanocomposite Cr_2O_3.

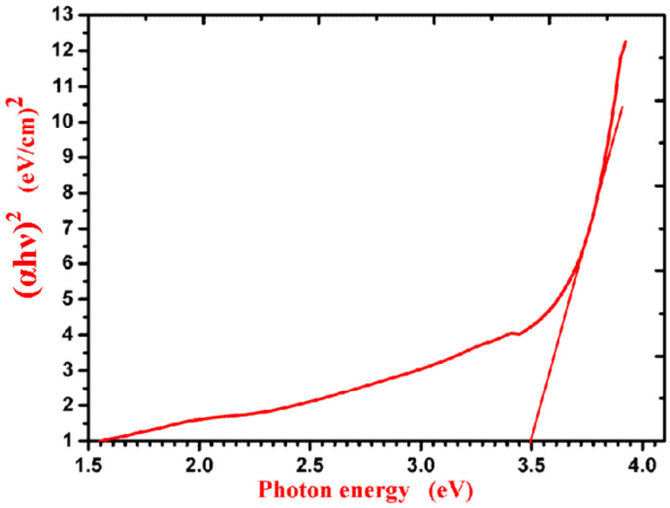

Figure 8: Direct transition for the nanocomposite.

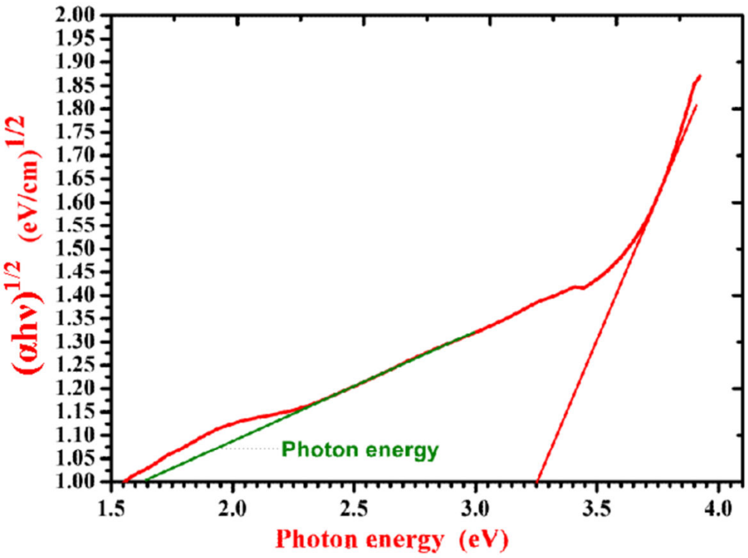

Figure 9: Indirect transition for the nanocomposite.

3.4. Transmittance analysis

Nanocomposite transmittance for all samples inspected by the SHIMADZU equipment in UV-IR wavelengths, the resulting showed that there is no transmittance for the nanocomposite for all samples during the tests. The Figure 10 showed the relationship drawn between the transmittance and the wavenumber for results test. The relation illustrates the transmittance start from the UV region as a 0.15 value and when it arrived at the visible region descended to zero value; this confirms that there is no transmittance and be as opaque materials. This nanocomposite when precipitated on the substrate doesn't permit the electromagnetic wavelengths as a solar energy to transmit through it [48, 49].

3.5. FT-IR analysis

The covalent bonds in molecules are not rigid sticks or rods, which is found in molecular kits in the crystalline lattice for the compounds but likes stiff springs that can be stretched and bent. The absorption spectra obtained of compounds that are a unique reflection of their molecular structure in the crystalline lattice. The absorption bands in the region from (400-900 cm^{-1}) are usually due to stretching vibrations of di-atomic units, and this is sometimes called the group frequency region, in the FT-IR spectra broad band of nanocomposite Cr_2O_3/C that precipitates on the substrates. The peaks of Cr-O bonds stretching vibration appears in Figure 11 shows sharp absorption bands falls at regions (489.9, 597.9, 659.6 and 785 cm^{-1}), respectively. In the present investigation, the observed peaks illustrate the peaks of Cr-O bond stretching vibration which be as a finger print of nanocomposite Cr_2O_3/C [50, 51].

3.6. Seebeck effect analysis

The Seebeck effect experiments found that if a piece of a composite is connected to a voltmeter by two metal connections, and one side of the composite is heated on the heated surface, and the other keeping in a cool surface then the galvanometer indicates that a current flows. From this thermoelectric effect was discovered during the experiment of the nanocomposite, whilst the results of the experiment were proved for this nanocomposite to be a semiconductor and the results exhibits a positive and negative resistance for each sample of nanocomposite that precipitated on the substrates. Then the Seebeck effect only appeared when two dissimilar metals are connected as a composite. There is a temperature difference be determined across the semiconductor of the nanocomposite recorded from the reading of the thermometers and the voltage difference reading by a voltmeter [52].

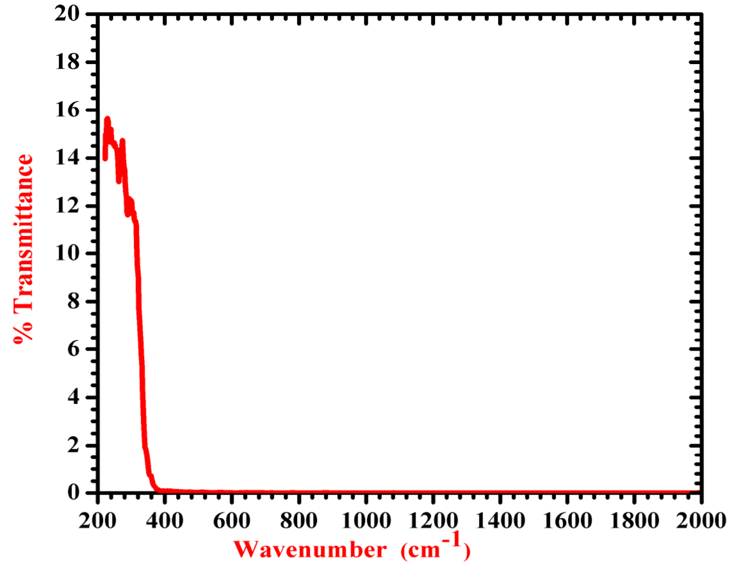

Figure 10: Nanocomposite transmittance.

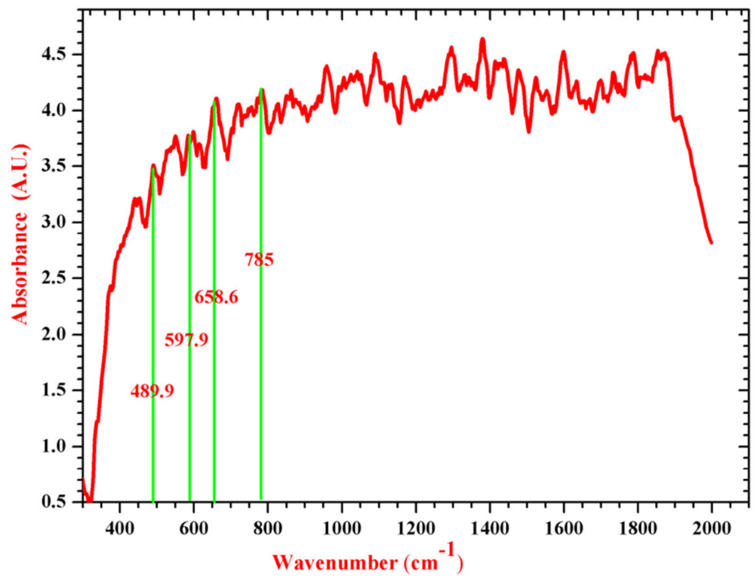

Figure 11: Nanocomposite finger print region.

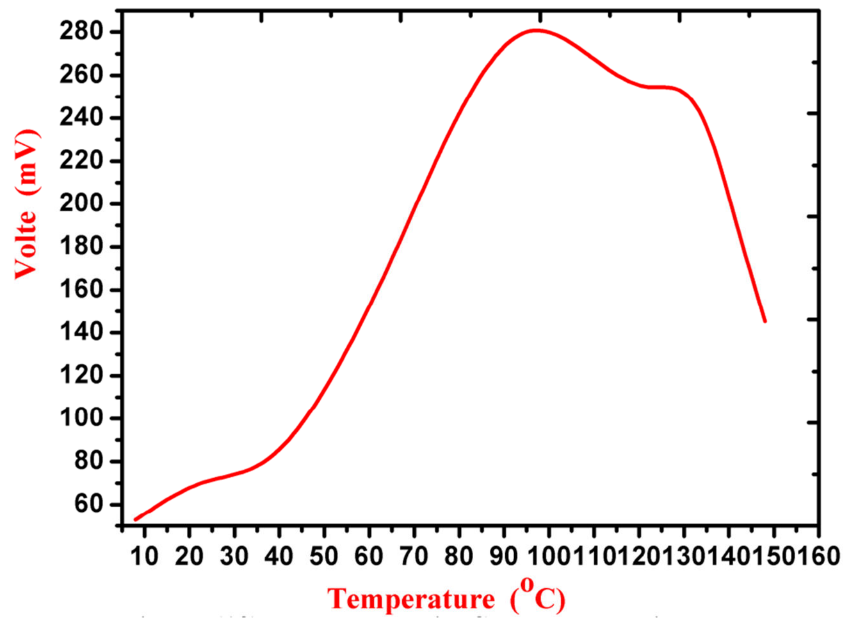

Figure 12: Nanocomposite Seebeck experiment.

Nanocomposite (Cr_2O_3/C) in Figure 12 exhibits the Seebeck effect diagram for the relation between the voltage difference and the temperature difference to gain the value of Seebeck effect and was between (960 to 6500 $\mu V\ K^{-1}$), from the results of the Seebeck effect prove that the nanocomposite (Cr_2O_3/C) was a semiconductor synthesis by spray coating method.

Finally, from the above results exhibited that carbon doped with nanomaterial Cr_2O_3 to be a nanocomposite Cr_2O_3/C. it is proved a semiconductor and has a good property toward the sun light. Thereby, it will be a good layer coating to absorb the solar energy, when utilized as a coating on the flat plate collector and absorbed the solar energy.

4. Conclusion

Carbon doped by nanoparticle Cr_2O_3 incorporated the photo-catalysts productivity; this created is solid and versatile for orchestrating Cr_2O_3 doped carbon photo-catalyst. The nanocomposite Cr_2O_3/C show high noticeable light photo-catalytic action, this action is approved of nanoparticle Cr_2O_3 to doping carbon particles. The band gap value in the table considering the incredible photo-catalytic created in an extensive variety of use in the solar energy. The experiments prove that the nanocomposite was a semiconductor manufactured in this research and be a good coating in the flat plate collector to absorb the solar energy in excellent way without any transmittance or reflectance of the solar energy from the surface of the flat plate collector, because this coating will be a trap to the solar energy. The values of the energy gaps were (3.5 and 3.25 eV) for direct and indirect transition, photon energy was 1.65 eV. The design and creation of a semiconductor structure based utilized as a part of spectrally selective coating (SSC). The nanocomposite Cr_2O_3/C is exceptionally for short-wavelength photons NIR and visible region for the semiconductor band gap. It found that the nanoparticle of Cr_2O_3 have essentially improved the solar absorptivity compared with uniform nanoparticles because of the more productive light trapping. The results of the band gap exhibited a good agreement with the other researcher and there is no transmittance for the nanocomposite. The FTIR analysis showed a good band stretching for the bond between the molecules of the nanocomposite. The Seebeck effect analysis proved that the nanocomposite was a semiconductor. Thin film thickness was around (45-150 µm) coincided with global company such as ALMECO company.

5. References

1. A. Basheer, Chemical chiral pollution: Impact on the society and science and need of the regulations in the 21st century, *Wiley J.*, 30(2018), 402-406.
2. A. A. Basheer, Imran Ali, Water photo splitting for green hydrogen energy by green nanoparticles, *Inter. J. Hydrogen Energy*, 44(2019), 11564-11573
3. Z. A. AL-Othman, A. Y. Badjah, I. Ali, Facile synthesis and characterization of multi walled carbon nanotubes for fast and effective removal of 4 tert octylphenol endocrine disruptor in water, *J. Mol. Liqu.*, 275(2019), 41–48.
4. I. Ali, New Generation Adsorbents for water treatment, *Am. Chem. Soc.*, 112(2012), 5073−5091.
5. I. Alia, A. A. Basheerc, X.Y. Mbiandad, A. Burakove, E. Galunine,I. Burakovae, E. Mkrtchyane, A. Tkacheve, V. Grachev, Graphene based adsorbents for remediation of noxious pollutants from wastewater, *Environ. Inter.*, 127(2019), 160–180
6. I. Ali, A. A. Basheer, A. Kucherova, N. Memetov, T. Pasko, K. Ovchinnikov, V. Pershin, D. Kuznetsov, E. Galunin, V. Grachev, A. Tkachev, Advances in carbon nanomaterials as lubricants modifiers, *J. Mol. Liq.*, 279(2019), 251-266.
7. A. A. Basheer, I. Ali, Water photo splitting for green hydrogen energy by green nanoparticles, *Inter. J. Hydrogen Energy*, 44(2019), 11564-11573
8. A. Fujishima, X. Zhang, D. A. Tryk, TiO_2 photocatalysis and related surface phenomena, *Surf. Sci. Rep.*, 63(2008), 515–582.
9. K. Hashimoto, H. Irie, A. Fujishima, TiO_2 photo-catalysis: a historical overview and future prospects, *Jpn. J. Appl. Phys.*, 44(2005), 8269–8285.
10. E. A. Burakova, T. P. Dyachkova, A. V. Rukhov, E. N. Tugolukov, E. V. Galunin, A. G. Tkachev, A. A. Basheer, I. Ali, Novel and economic method of carbon nanotubes synthesis on a nickel magnesium oxide catalyst using microwave radiation, *J. Mol. Liq.*, 253(2018), 340–346.
11. I. Ali and C. K. Jain, Advances in arsenic speciation techniques, *Intern. J. Environ. Anal. Chem.*, 84(2004), 947–964.
12. I. Ali, Z. A. AL-Othman, M. M. Sanag, Green synthesis of iron nano-impregnated adsorbent for fast removal of fluoride from water. *J. Mol. Liq.* 211(2015), 457–465.
13. I. Ali, Z. A. Alothman, A. Alwarthan, Uptake of propranolol on ionic liquid iron nanocomposite adsorbent: kinetic, thermodynamics and mechanism of adsorption, *J. Mol. Liq.*, 236(2017), 205-213.
14. I. Ali, O. M.L. Alharbi, Z. A. Alothman, A. Y. Badjah, A. Alwarthan, A. A. Basheer, Artificial neural network modelling of amido black dye sorption on iron composite nanomaterial: Kinetics and thermodynamics studies. *J. Mol. Liq.* 250(2018), 1–8.
15. J. Xu. J. J. Zhu, H. Wang, H. Y. Chen, Nano-sized copper oxide modified carbon paste electrodes as an amperometric sensor for amikacin. *Anal. Lett.* 36(2003), 2723-2733.
16. V. Pillai, P. Kumar, M. J. Hou, P. Ayyub, D. O. Shah, Preparation of nanoparticles of silver halides, superconductors and magnetic materials using water-in-oil microemulsions as nano-reactors. *Adv. Colloid Inter. Sci*. 55(1995), 241-269.
17. I. Ali, Microwave assisted economic synthesis of multi walled carbon nanotubes for arsenic species removal in water: Batch and column operations, *J. Mol. Liq.*, 271(2018), 677-685.
18. I. Ali, O. M. L. Alharbi, Z. A. Alothman, A. Alwarthan, Facile and eco-friendly synthesis of functionalized iron nanoparticles for cyanazine removal in water, *Colloid. Surface B*, 171(2018), 606-613.
19. I. Ali, O. M. L. Alharbi, Z. A. Alothman, A. Y. Badjah, Kinetics, thermodynamics and modelling of amido black dye photodegradation in water using Co/TiO_2 nanoparticles, *Photochem. PhotoBiol.*, 94(2018), 935-941.
20. I. Alia, O. M. L. Alharbi, Z. A. ALothman, A. M. Al-Mohaimeed, A. Alwarthan, Modeling of fenuron pesticide adsorption on CNTs for mechanistic insight and removal in water, *Environ. Res.*, 170(2019), 389–397.
21. I. Ali, Z. A. Al-Othman and A. Al-Warthan, Removal of secbumeton herbicide from water on composite nanoadsorbent, *Desalin. Water Treat.*, 57(2016), 10409-10421.
22. Z. Yang, X. Peng, C. Xu, F. Wang, Electrochemical assembly of Ni–xCr–yAl nano composites with excellent high-temperature oxidation resistance, *J. Electrochem. Soc.*, 156(2009), C167-C175.
23. H. Rotter, M. V. Landau, M. Carrera, d. Gold farb, M. Herskowitz, Spectral Tuning in the Human Blue Cone Pigment, *Biochem.*, 38(1999), 11593–11596.
24. R. H., L. M. V., C. M., G. D., H. M., High surface area chromia aerogel efficient catalyst and catalyst support for ethylacetate combustion, Appl. Catal. B, 47(2004), 111-126.
25. C. L., S. Z., W. X., P. S. V., Hu J., K. S., R. R., Three-dimensional morphology control during wet chemical synthesis of porous chromium oxide spheres, *Appl. Mater. Interface*, 1(2009), 1931–1937.
26. W. S. Chae, S. W. Lee, Y. R Kim, Templating route to mesoporous nanocrystalline titania nanofibers. *Chem. Mater.* 17(2005), 3072-3074.
27. Y. W. Jun, M. F. Casula, J. H. Sim, S. Y. Kim, J. Cheon, A. P. Alivisatos, Surfactant-assisted elimination of a high energy facet as a means of controlling the shapes of TiO_2 nanocrystals. *J. Am. Chem. Soc.* 125(2003), 15981-15985.
28. Z. Zhang, C. C. Wang, R. Zakaria, J. Y. Ying, Role of particle size in nano crystalline TiO_2-based photo-catalysts. *J. Phys. Chem. B*. 102(1998), 10871-10878.

29. S. Kim, S. J. Hwang, W. Choi, Visible light active platinum-ion-doped TiO_2 photocatalyst. *J. Phys. Chem. B.* 109(2005), 24260-24267.
30. Y. Choi, T. Umebayashi, S. Yamamoto, S. Tanaka, Fabrication of TiO_2 photo-catalysts by oxidative annealing of TiC. *J. Mater. Sci. Lett.* 22(2003), 1209-1211.
31. Z. Wu, The fabrication and characterization of novel carbon doped TiO_2 nanotubes, nanowires and nanorods with high visible light photocatalytic activity. *Nanotechnol.* 20(2009), 235701-235710.
32. R. Bechstein, Evidence for vacancy creation by chromium doping of rutile titanium dioxide (110). *J. Phys. Chem. C*. 113(2009), 3277–3280.
33. G. K. Larsen, Structural, optical, and photocatalytic properties of Cr: TiO_2 nanorod array fabricated by oblique angle Co-deposition, *J. Phys. Chem. C*, 115(2011), 16892–16903.
34. R. Bhosale, Visible-light-activated nano composite photo-catalyst of Cr_2O_3/SnO_2. *J. Nanostructure Chem.* 3 (2013), 1-8.
35. A. Hajjaji, Photocatalytic activity of Cr-doped TiO_2 nanoparticles deposited on porous multi crystalline silicon films. *Nanoscale Res. Lett.* 9(2014), 1-6.
36. S. Guan, Fabrication of photocatalyst composite coatings of Cr-TiO_2 by mechanical coating technique and oxidation process, *Coatings*, 5(2015), 545-556.
37. H. Yan, Band structure design of semiconductors for enhanced photocatalytic activity: the case of TiO_2. *Prog. Natural Sci. Mater. Int*. 4(2013), 402–407.
38. M. K. Alamgir, Tailoring the energy band gap of transition metal doped TiO_2 thin film. *J. Nano Anal.* 3(2014), 129-134.
39. E. Kim, Measurement and calculation of optical band gap of chromium aluminum oxide films. *Jpn. J. Appl. Phys.* 39(2000), 4820–4825.
40. S. M. Sabnis, P. A. Bhadane, P. G. Kulkarni, Process flow of spray pyrolysis technique, *IOSR J. Appl. Phy.* 4(2013), 7-11.
41. B. Okolo, P. Lamparter, U. Welzel, E. J. Mittemeijer, Stress, texture, and microstructure in niobium thin films sputter deposited onto amorphous substrates. *J. Appl. Phys.* 95(2004), 466-473.
42. M. Tabbal, S. Kahwaji, T.C. Christidis, B. Nsouli , K. Zahraman, Pulsed laser deposition of nanostructured dichromium trioxide thin films. *Thin Solid Films*. 515(2006), 1976-1984.
43. T. K. Hamad, Refractive index dispersion and analysis of the optical parameters of (PMMA/PVA) thin film. *J. Al-Nahrain Univer.* 16(2013), 164-170.
44. A. Ali, D. Fadhil, E. Yousif, Z. Hussain, S. Abdul-Wahab, A comprehensive study of *conductive polymer matrix composites: A review, Res. J. Pharmac. Biological Chem. Sci*. 8(2017), 2043- 2049.
45. R. N. Abed, N. K. Al-Sahib and A. N. Khalifa, Optical study to doping carbon with TiO_2 that utilizing in thermal concentration. *Oriental J. Phy. Sci.*, 2(2017), 109-113.
46. M. Julkarnain, J. Hossain, K. S. Sharif, and K. A. Khan, Optical properties of thermally evaporated Cr_2O_3 thin films. *Canadian J. Chem. Eng. Technol.*, 3(2012), 81-85.
47. T. Ivanova, K. Gesheva, A. Cziraki, A. Szekeres and E. Vlaikova, Structural transformations and their relation to the optoelectronic properties of chromium oxide thin films. *J. Phys. Conference Ser.*, 113(2008), 1-5.
48. A. Elwhab B. Alwany, O. M. Samir, M. A. Algradee, M. M. Hafith, M. A. Abdel-Rahim, Investigation of the effect of film thickness and heat treatment on the optical properties of TeSeSn thin films. *World J. Condensed Matter Phys.* 5(2015), 220-231.
49. N. G. Ndegwa, F. G. Ndiritu, A. S. Hussein, P. K. Kamweru, J. K. Kagia, Z. W. Muthui, Reflectance, transmittance and absorptance of HDPE, LDPE, glass and sand layer used in a SAH. *Inter. J. Appl. Phys. Mathem*. 4(2014), 406-4016.
50. M. M. Abdullah, F. M. Rajab, S. M. Al-Abbas, Structural and optical characterization of Cr_2O_3 nanostructures: evaluation of its dielectric properties. *Am. Institute Phys. Adv.* 4(2014), 1-11.
51. M. Diantoro, M. B. Zaini, Z. Muniroh, N. Ahidayat, The effect of Cr_2O_3 doping on structures and dielectric constants of SiO_2-Bi_2O_3-B_2O_3-Na_2CO_3 glass based on silica gel of natural sand, International Conference on Physical Instrumentation and Advanced Materials, *J. Phys. Conf. Series*. 853(2017), 1-9.
52. J. Jenkins, W. H. Jarvis, W. Ashhurst, basic principles of electronics, vol. 2, Semiconductors book, Elsevier, 1971.

How to cite this article:

R. N. Abed, N. K. Al-Sahib, A. J. N. Khalifa, Energy Gap Demeanor for Carbon Doped with Chrome Nanoparticle to Increase Solar Energy Absorption. Prog. Color Colorants Coat., 13 (2020), 143-154.